Макрогетероциклы
http://mhc-isuct.ru

DOI: 10.6060/mhc256557k

# On the Conductivity of Carbon Nanotubes and Their Composites with Polymeric Phthalocyanines

Ivan Yu. Kurochkin,[a] Galina G. Ryzhkova,[a,b] Alena A. Mitina,[a@]
Tatiana N. Rudneva,[a] Vladimir A. Radnev,[a] Andrey V. Moiseenko,[c]
Maxim A. Knyazev,[a] Evgene E. Yakimov,[a] and Vitaly I. Korepanov[a]

[a]*Institute of Microelectronics Technology and High Purity Materials RAS, 142432 Chernogolovka, Russia*
[b]*Samara National Research University, 443086 Samara, Russia*
[c]*Faculty of Biology, Lomonosov Moscow State University, 119991 Moscow, Russia*
[@]*Corresponding author E-mail: alena@iptm.ru*

Dedicated to Corresponding Member of the Russian Academy of Sciences G. N. Vorozhtsov on the occasion of his 90th Anniversary

*Polymeric iron phthalocyanine (FePPC) and its composites with single-walled and multi-walled carbon nanotubes (FePPC@SWCNT and FePPC@MWCNT) were synthesized. The conductivity of FePPC and its composites was then studied and compared to pristine SWCNT, MWCNT and mononuclear iron phthalocyanine (FePC). Both FePPC and FePC exhibited semiconductor-like behavior with sub-eV activation energies; however, the polymer demonstrated significantly higher conductivity than its mononuclear counterpart. In the composites, the presence of the polymer substantially altered the conductivity. The charge transport in FePPC@CNT composites is of major importance for electrocatalytic systems based on carbon nanotubes and conductive polymers.*

**Keywords:** Carbon nanotubes, iron polyphthalocyanine, composites, conductivity.

# О проводимости углеродных нанотрубок и их композитов с полимерными фталоцианинами

И. Ю. Курочкин,[a] Г. Г. Рыжкова,[a,b] А. А. Митина,[a@] Т. Н. Руднева,[a]
В. А. Раднев,[a] А. В. Моисеенко,[c] М. А. Князев,[a] Е. Е. Якимов,[a] В. И. Корепанов[a]

[a]*Федеральное государственное бюджетное учреждение науки Институт проблем технологии микроэлектроники и особочистых материалов Российской академии наук ИПТМ РАН, 142432 Черноголовка, Россия*
[b]*Самарский национальный исследовательский университет имени академика С.П. Королева, 443086 Самара, Россия*
[c]*МГУ имени М.В. Ломоносова, Кафедра биоинженерии (Биологический факультет), 119991 Москва, Россия*
[@]*E-mail: alena@iptm.ru*

*Мы синтезировали полимерный фталоцианинат железа (FePPC) и получили его композиты (FePPC@CNT) с одностенными (SWCNT) и многостенными (MWCNT) углеродными нанотрубками. Далее мы изучили поведение проводимости полимера с SWCNT, MWCNT и композитами на их основе, а также с моноядерным фталоцианином (FePC). Как полимер FePPC, так и FePC показывают полупроводниковое поведение с энергиями активации ниже эВ. Полимер показывает гораздо более высокую проводимость, чем его моноядерный аналог. В композите полимер вызывает выраженные изменения проводимости. Транспорт заряда в системах, таких как композит FePPC@CNT, имеет большое значение в электрокаталитических системах на основе углеродных нанотрубок и проводящих полимеров.*

**Ключевые слова:** Углеродные нанотрубки, полифталоцианинат железа, композиты, проводимость.

  

## Introduction

Although carbon nanotubes (CNTs) possess high electrical conductivity, their performance in various applications can be significantly enhanced by the addition of functional components. One of the common ways to modify CNTs is a polymer wrapping. The use of polymers in CNT-based materials allows one to adjust a number of important properties, such as conductivity, transparency and flexibility and their combinations.[1,2] Polymers also can be used in creating stable suspensions of CNTs.[3] Variation of the polymer allows control of the electrical properties of such materials. The wrapping can be implemented through different types of non-covalent interactions (π-π stacking, CH-π interaction and cation-π interaction), which preserves the intrinsic properties of the CNTs.

A wide range of applications for CNTs is achieved by using polymers of different natures. One of the most promising types of CNT composites can be created by using 2D-conjugated polymers, metal polyphthalocyanines (PPC) (Figure 1). The π-electronic conjugation makes phthalocyanines conductive. PPCs themselves are promising candidates for a variety of applications such as spintronics, magnetic storage devices[4,5] and memristor devices.[6] PPC@CNT composites are especially promising in electrocatalysis[7–10] and sensorics.[11]

Both mononuclear phthalocyanines (PC) and polymeric phthalocyanines are used to modify CNTs, but the polymer form has a number of advantages. PPCs are expected to exhibit higher conductivity and a lower band gap than mononuclear PCs due to the extended π-electron conjugation in the polymer.[12] While the quantum-chemical calculations estimate the band gap of PPCs to be about 0 eV,[13,14] the real bulk material has a semiconductor-like charge transport behavior with a distinct activation energy for the charge transport.[15] The main advantage of PPCs over PCs is a high chemical and thermal stability.[6] This also significantly increases the resistance of the hybrid material to acids.[7] In another work it was shown that due to an enhanced delocalization of π electrons in PPC conjugation system NiPPC@CNT composites show a higher activity and stability for $CO_2$ reduction comparison to NiPC/CNT.[16] A key disadvantage of these polymers is their poor processability, as PPCs are generally insoluble and non-volatile. There are two possible pathways to solve the processability problem: (1) processing PPCs into functional inks for printable electronics and (2) using PPCs in various composites (for example with CNTs). The present work is focused on the second approach.

PPC@CNT composites can be prepared in several ways. In the work [7], the synthesis was done by microwave heating of pre-oxidized MWCNT, 1,2,4,5-tetracyanobenzene and $FeCl_2$ in pentanol at 180 °C. Xu and coworkers prepared InPPC@CNT in two steps by first making InPPC dispersion in ethanol (autoclave, 160 °C) and next adsorbing InPPC on CNT in DMF.[10] A similar procedure was used by Duan and coworkers, who did the synthesis directly in ethanol at 180 °C in presence of a catalyst (DBU).[17] All reported approaches employ low-temperature synthesis, which likely yields a material with a low degree of polymerization. After the formation of the first PC ring, the following steps of the chemical reaction require higher activation energy and therefore higher temperatures (above 350 °C [9]). It is interesting therefore to try a high-temperature synthesis for making such composites. Such synthesis was one of the aims of the present work.

In SWCNT and MWCNT-based materials, the electrical conductivity depends on a number of factors: the CNT concentration (whether a percolation network is formed), the ratio of geometric parameters of CNT (diameter/length),[18,19] morphology of the CNT network,[20,21] doping;[22] in the polymer composites also on the type of the polymer.[23–25] Besides, even pristine SWCNTs may exhibit metallic or semiconducting properties depending on their structure.[19] Consequently, SWCNTs can exhibit different temperature-dependent resistance behaviors: the resistance of metallic nanotubes should increase with temperature, while for semiconducting it should decrease.[26] The polymer in composites also may have its specific conductivity behavior.

Depending on intrinsic parameters of CNTs and the form of the sample (powder/thin film/fiber/bulk paper), the measured conductivity value can vary within several orders of magnitude.[27] For commercial SWCNT or MWCNT powders typical values are $10^3$–$10^5$ S/m (but typically vendors do not provide the conditions at which these values were measured). As shown in the works,[28,29] the conductivity has a strong dependence on the pressure. Sometimes lower values can be found in the literature, for example upon increasing pressure up to ~17 MPa the conductivity of the MWCNT powder changes from 0.5 to 800 S/m.[28] These examples demonstrate that direct comparisons of literature data are often meaningless. The comparison of the resistivity values is meaningful only at comparable pressures.[30] The fact that for polymeric phthalocyanines reliable conductivity measurements are practically absent in the literature was also one of the motivations of the present work.

A typical set-up for estimation of resistivity is described in the work [31]. It basically consists of two contacts, between which the carbon sample is pressed at some fixed pressure. The aim of the present work was to obtain composites of iron polyphthalocyanine (FePPC) with carbon nanotubes and test their charge transport behavior as compared to original CNTs, FePPC and mononuclear FePC.

## Experimental

### *Materials*

Commercial reagents 1,2,4,5-tetracyanobenzene (TCB, 97%, Sigma-Aldrich Chemical Co, India), ferrocene (98%, Merck, Germany), mononuclear phthalocyanine (FePC, 96%, Alfa Aesar, USA), dimethyl sulfoxide (DMSO, 99.5%, EKOS-1, Russia) and methanol (for gradient HPLC, Chimmed, Russia) were used without additional purification. Singlewall carbon nanotubes (SWCNT) were purchased from OCSiAl (Novosibirsk, Russia); according to the manufacturer, the average diameter was ~1.6±0.15 nm; their detailed characterization can be found in the literature.[32] Argon gas (99.999%), was supplied by "Linde gas" (Russia).

### *Synthesis*

*Multiwall carbon nanotubes (MWCNT)* were synthesized by chemical vapor deposition (CVD) according to the previously developed method.[33] Nickel nitrate hexahydrate ($Ni(NO_3)_2{\cdot}6H_2O$) powder was used as the catalyst precursor. The synthesis procedure was as follows. A powder of $Ni(NO_3)_2{\cdot}6H_2O$ was ground in a

mortar and then spread in a thin layer on the surface of a quartz boat covered with aluminum foil. The boat containing the precursor was placed in the reactor. Ethanol (96 wt.%, Russia) was used as the carbon source. The decomposition of the catalyst precursor was carried out in ethanol vapour. The synthesis temperature was 600 °C and the deposition time was 1 h. The process was carried out at atmospheric pressure without using a carrier gas.

*Iron polyphthalocyanine (FePPC)* was synthesized by sintering TCB with ferrocene via a procedure similar to the previously reported [34]. TCB and ferrocene in a molar ratio of 2:1 were thoroughly ground and mixed in a mortar. The mixed powder in a quartz crucible was placed in a tube furnace. The mixture was calcined at 460 °C under a flow of argon (~1 l/hr) with a constant injection of methanol from the top side of the reactor at a speed of 0.125 ml/min. After the methanol feed (total 20 ml) was finished, the furnace was cooled to room temperature under a flow of argon. The black solid was obtained. The resulting solid was ground into powder in a mortar and washed with DMSO, methanol and water to remove unreacted ferrocene and phthalocyanine oligomers.

*Composites of iron polyphthalocyanine with SWCNT* were prepared similarly to FePPC synthesis, with addition of SWCNT (same mass as ferrocene) to the mixture of TCB and ferrocene.

*Composites of iron polyphthalocyanine with MWCNT* were prepared similarly to FePPC synthesis, with addition of MWCNT (same mass as ferrocene) to the mixture of TCB and ferrocene.

The yield, determined from the amount of polymer formed, was over 70% for all syntheses.

## *Characterization*

*Energy Dispersive X-Ray Spectroscopy (EDX).* The measurements were carried in the scanning electron microscope JSM 6490 (Jeol) equipped with the Oxford Instruments INCAx-sight energy dispersive system. The beam energy was of 20 keV and the beam current about $10^{-10}$ A.

*Raman spectra* were measured with a Bruker Senterra micro-Raman system under 532 nm excitation and laser power 0.1 mW with 50x objective and 2x60s acquisition time.

*Two-piston method.* The lab-built set-up was used for conductivity measurements. The scheme was similar to the one reported in the work [31]: setup had two cylindrical brass electrodes (5 mm in diameter) that were linked to a Keithley 2000 digital multimeter and contained within the ceramic tube. A spiral coil band heater was used for heating the ceramic tube. The upper electrode was hollow and sealed at one edge. A thermocouple was placed in it to measure the temperature close to the sample. The Keithley 2000 was utilized in the 4-wire resistance measuring mode, which has a basic resistance accuracy of 0.008%. A different multimeter, the AKTACOM AM-1109, was used to record the DC voltage (accuracy of 0.06%). The samples were put between the electrodes in powdered form (100 mg per sample). While the temperature was changing at a rate of 5 degrees per minute, a steady pressure of roughly 0.56 MPa was maintained. Although the dispersity of the samples was not thoroughly examined, scanning electron microscopy (SEM) examinations provide an approximate estimate that the powders are made up of particles ranging in size from hundreds of nm to tens of microns (Figure S1, *Supporting Information*).

*Transmission electron microscopy (TEM) images* were obtained from suspensions deposited on TEM grids. 3 µl of sample suspension (with SDBS as a surfactant) were applied to the hydrophilized lacey carbon film (TedPella, USA) and dried at room temperature. The images were acquired with JEM-2100 transmission electron microscope (JEOL, Japan) equipped with Orius SC200D camera (Gatan, USA) and DE-20 camera (Direct Electron, USA).

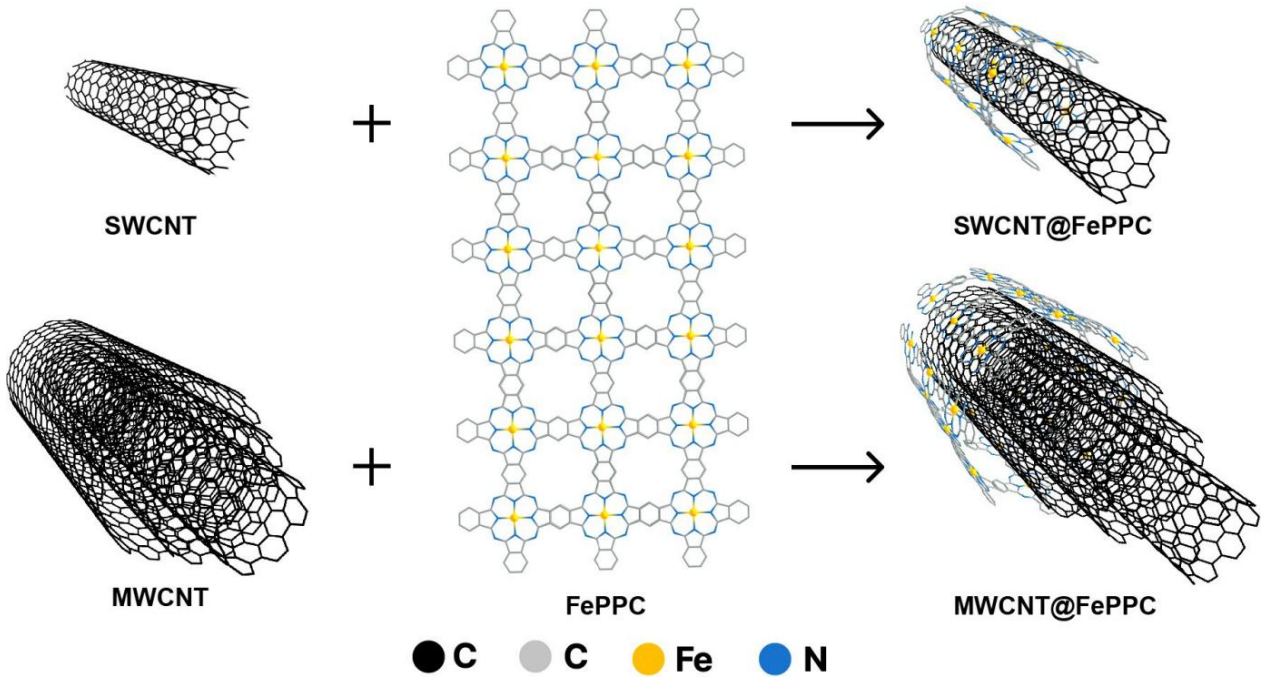


**Figure 1**. General scheme for the preparation of PPC@CNT composites. In the present work, FePPC was formed *in situ* from tetracyanobenzene.

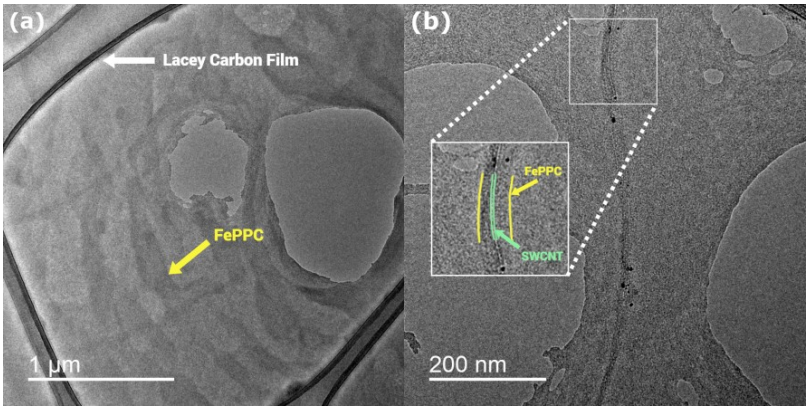


**Figure 2.** TEM images of FePPC (a) and FePPC@SWCNT composite (b). The lacey carbon film is visible on the left image. FePPC with SDBS forms a thick film that is sensitive to the electron beam. On the right image the PPC-wrapped CNTs are suspended in SDBS film.

## Results and Discussion

Transmission electron imaging (TEM) shows that the polymer (FePPC) has a layered structure (Figure 2a). For FePPC@SWCNT, composite fibers are significantly thicker than the original CNTs. In the centre of the fiber, a thin CNT can be identified (Figure 2b). This suggests that during the synthesis the nanotubes were wrapped with several layers of polymer, and confirms the formation of a composite rather than a mechanical mixture. It is difficult to confirm the structure of the FePPC@MWCNT composite using TEM, since the MWCNT themselves have multiple layers, and it is difficult to make a reliable distinction between the CNT walls and the polymer coating.

For FePPC, EDX measurements, within the precision limits of the method, are in reasonable agreement with the expected structure. Values from the structural formula of the polymer: C:N:Fe = 20:8:1; found values: C:N:Fe = = 20:12.8:0.25. Due to overlapping of carbon and nitrogen peaks and the method's intrinsic accuracy (~1%), the nitrogen content has additional uncertainty from peak fitting and should be considered approximate. The metal content is below stoichiometric values, consistent with literature reports [8] of partial metal vacancies in the lattice.

Raman spectra of nanotubes, composites and phthalocyanines are shown in Figure 3. When comparing the spectra of FePPC and FePC, it can be seen that in the case of the polymer, the spectrum has broader bands, and less features below 1000 $cm^{-1}$ (the latter are attributed mostly to monomeric phthalocyanine[35]). The peak at 690 $cm^{-1}$ in both spectra corresponds to phthalocyanine macrocycle breathing mode.[36] The minor peak at ~2220 $cm^{-1}$ in the spectra of FePPC and composites comes from the terminal groups (CN triple bond). The broad features in the 1000–1700 $cm^{-1}$ range in the polymer's spectrum are attributed to a significantly higher degree of π-conjugation in FePPC compared to FePC.[9] In FePPC@SWCNT and FePPC@MWCNT spectra FePPC peaks are clearly visible, but it is difficult to detect nanotube peaks, because D and G bands of CNTs are in the same range as the FePPC peaks, and, probably, CNTs are screened from the excitation laser by the polymer.

Resistivity values of the studied compounds are given in Table 1 for different temperature conditions. Temperature dependences of reduced resistances ($R/R_{300\,K}$) and calculated $E_a$ are shown in Figure 4. Here, $E_a$ was estimated by linearization of the plot with the following equation:

$$ln\left(\frac{R}{R_{300K}}\right) = \frac{E_a}{k_B} \cdot \frac{1}{T}$$

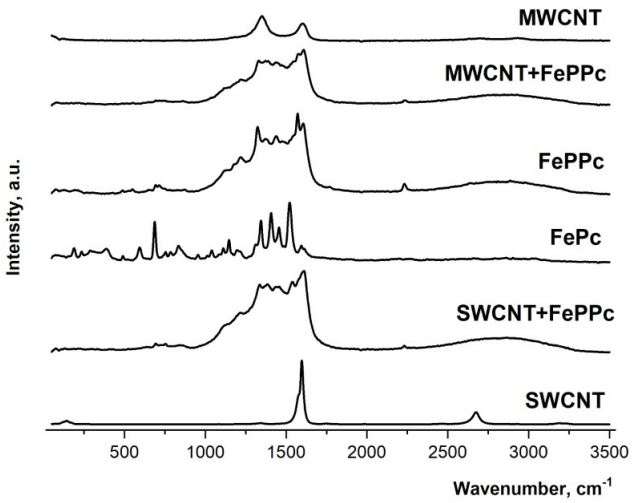


**Figure 3.** Raman spectra of iron(poly)phthalocyanine, carbon nanotubes and their composites.

**Table 1**. Electrical properties of the samples.

| Sample | $R_{300\,K}$, Ω | $R_{410\,K}$, Ω | $E_a$, eV |
|---|---|---|---|
| FePC | $3.7 \cdot 10^6$ | $5.6 \cdot 10^4$ | 0.38 |
| FePPC | $3.9 \cdot 10^5$ | $1.3 \cdot 10^4$ | 0.27 |
| SWCNT | 1.7 | 1.4 | 0.03 |
| MWCNT | 8.4 | 2.6 | 0.12 |
| FePPC@SWCNT | 8.4 | 2.5 | 0.11 |
| FePPC@MWCNT | $3.2 \cdot 10^4$ | $1.9 \cdot 10^3$ | 0.23 |

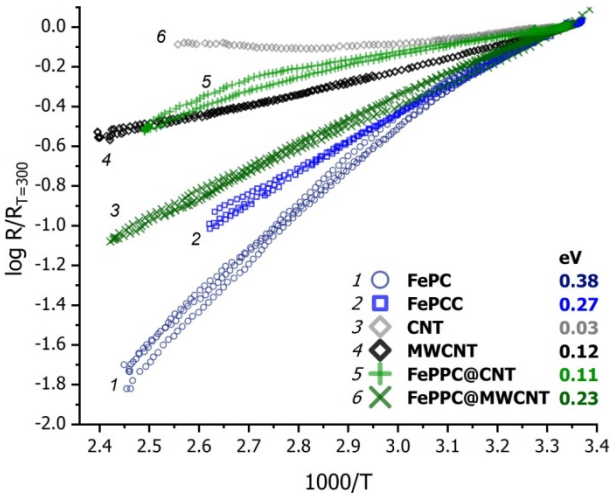


**Figure 4**. Temperature dependence of electrical resistance of FePC (circle), FePPC (square), SWCNT (gray diamond), MWCNT (black diamond), FePPC@SWCNT (cross +), FePPC@MWCNT (cross ×). Dependency points were recorded both during heating and cooling of the samples.

The polymer (FePPC) exhibits a resistivity one order of magnitude lower than that of mononuclear FePC at 300 K. The charge transport activation energy derived from the Arrhenius plot is also lower for FePPC than for FePC (0.27 vs 0.38 eV).

Semiconducting behavior is common for both PCs and PPCs, regardless of the material form (powder, thin film or composite component), as demonstrated in a number of works.[12,15,37,38] For both monomeric[37] and polymeric[39] phthalocyanines, the *p*-type semiconductivity was reported. For the charge transport activation energy ($E_a$) and the activation energy of conduction of FePC and FePPC, significantly different values were reported in the literature,[12,15,37,38] ranging from 0.1 to 0.7 eV. However, lower $E_a$ values should correspond to PPCs compared to their PCs analogs. Energy gaps of polymers should decrease upon the increase of the number of the conjugated rings.[40]

The powder of both CNT types is by orders of magnitude more conductive than FePC or FePPC, and possess significantly lower $E_a$ values. These observations fit expectations and agree well with literature data.[41] For CNTs, $E_a$ values from 0.23 eV to 0 eV were reported in the literature.[21,41,42] CNTs can exhibit conductive properties close to metals depending on the sample. In our measurements, the $E_a$ of 0.12 eV was obtained for MWCNT powder, while the resistance of SWCNT cannot be well described by the linear curve on the Arrhenius plot (Figure 4), therefore the value of ~0.03 eV should be interpreted as metallic conductivity.

The FePPC@SWCNT and FePPC@MWCNT composite powders demonstrated higher conductivity than PC and PPC but lower than that of pristine CNTs. The composites derived from MWCNT and SWCNT exhibit significantly different electrical properties: resistance of FePPC@MWCNT is ~3 orders of magnitude higher than that of FePPC@SWCNT. Interestingly, FePPC@CNT showed charge transport properties (both $E_a$ and conductivity) very close to those of MWCNT. Charge transport measurements show that for both types of composites, the polymer has a high impact on the conductivity. The composite likely possesses a complex structure, the conductivity of which has three major contributions: metallic-like from CNTs, semiconducting from PPCs and (probably, also semiconducting) from the junctions between the macromolecules. The literature data suggest that the performance of such complex structures is dominated by junctions and related barriers.[20,43] The absence of metallic conductivity in the FePPC@CNT composites further confirms the formation of a composite structure in which the nanotubes are wrapped by the polymer. Although we do not have direct evidence, the major mechanism of the polymer/CNT interaction is probably the enhanced π-π stacking, since both CNTs and 2D conjugated polymers have extended π-systems.

## Conclusions

Polymeric iron phthalocyanine (FePPC) exhibits semiconductor-like charge transport properties. FePPC has a lower charge transport activation energy and higher conductivity than its mononuclear analog (FePC), which is interpreted as a direct consequence of extended electronic conjugation in the polymer.

The composites likely feature a complex electronic structure comprising CNTs, PPCs, and the junctions between the macromolecules. In composites of FePPC with carbon nanotubes the polymer alters the conductivity, turning the charge transport to semiconductor-like behavior with low sub-eV activation energy.

The PPC@CNT composites are highly promising materials for electrocatalysis and sensors, therefore their charge transport behavior is of high practical importance.

**Acknowledgements.** This research was funded by the Russian Science Foundation (project number 24-22-00240). TEM measurements were carried out at the Shared Research Facility “Electron microscopy in life sciences” at Moscow State University (Unique Equipment “Three-dimensional electron microscopy and spectroscopy”).

**Author contributions.** Ivan Yu. Kurochkin: investigation, writing – original draft; writing – review and editing; Galina G. Ryzhkova: investigation, methodology; writing – original draft; writing – review and editing; Alena A. Mitina: investigation, funding acquisition; supervision, writing – original draft, writing – review and editing; Tatiana N. Rudneva: investigation, writing – original draft; writing – review and editing; Vladimir A. Radnev: investigation, methodology, visualization; Andrey V. Moiseenko: investigation, visualization, writing – original draft; writing – review and editing; Maxim A. Knyazev: investigation, writing – original draft; writing – review and editing; Evgene E. Yakimov: investigation, writing – original draft; writing – review and editing; Vitaly I. Korepanov: conceptualization, investigation, writing – original draft, writing – review and editing.

## References

1. Cai L., Wang C. *Nanoscale Res. Lett.* **2015**, *10*, 1–21. doi: 10.1186/s11671-015-1013-1
2. a) Hu B., Li D., Manandharm P., Fan Q., Kasilingam D., Calvert P. *J. Mater. Chem.* **2011**, *22*, 1598–1605. doi: 10.1039/C1JM14121J; b) Kozlov G.V., Dolbin I.V. *ChemChemTech* **2022**, *65*(1), 38–43. doi: 10.6060/ ivkkt.20226501.6389

3. Fujigaya T., Nakashima N. *Sci. Technol. Adv. Mater.* **2015**, *16*, 024802. doi: 10.1088/1468-6996/16/2/024802
4. Zhou J., Sun Q. *J. Am. Chem. Soc.* **2011**, *133*, 15113–15119. doi: 10.1021/ja204990j
5. Wang P., Jiang X., Hu J., Huang X., Zhao J. *J. Mater. Chem. C* **2016**, *4*, 2147–2154. doi: 10.1039/c5tc04402b
6. Guo X., Liu J., Cao L., Liang Q., Lei S. *ACS Omega* **2019**, *4*, 10419–10423. doi: 10.1021/acsomega.9b01224
7. Wang X., Wang B., Zhong J., Zhao F., Han N., Huang W., *et al. Nano Res.* **2016**, *9*, 1497–1506. doi: 10.1007/s12274-016-1046-5
8. Zhang Y., Zhang X., Jiao L., Meng Z., Jiang H-L. *J. Am. Chem. Soc.* **2023**, *145*, 24230–24239. doi: 10.1021/jacs.3c08594
9. Sedlovets D.M., Volkov V.T., Khodos I.I., Zotov A.V., Korepanov V.I. *J. Phys. D: Appl. Phys.* **2019**, *52*, 245303. doi: 10.1088/1361-6463/ab1382
10. Xu Y., Zhu X., Ran L., Li X., Chen S., Qiu X. *Chem. Eng. Sci.* **2024**, *287*, 119749. doi: 10.1016/j.ces.2024.119749
11. Shao W., Mai J., Wei Z. *Chemosensors* **2022**, *10*, 83. doi: 10.3390/chemosensors10020083
12. Norrell C.J., Pohl H.A., Thomas M., Berlin K.D. *J. Polym. Sci., Part B: Polym. Phys.* **1974**, *12*, 913–924. doi: 10.1002/pol.1974.180120506
13. Sedlovets D.M., Shuvalov M.V., Vishnevskiy Y.V., Volkov V.T., Khodos I.I., Trofimov O.V., *et al. Mater. Res. Bull.* **2013**, *48*, 3955–3960. doi: 10.1016/j.materresbull.2013.06.015
14. Han N., Wang Y., Ma L., Wen J., Li J., Zheng H., *et al. Chem.* **2017**, *3*, 652–664. doi: 10.1016/j.chempr.2017.08.002
15. Inoue H., Kida Y., Imoto E. *Bull. Chem. Soc. Jpn.* **1968**, *41*, 684–691. doi: 10.1246/bcsj.41.684
16. Chen K., Cao M., Ni G., Chen Sh., Liao H., Zhu L., Li H., Fu J., Hu J., Cortés E., Liu M. *Appl. Catal. B* **2022**, *306*, 121093. doi: 10.1016/j.apcatb.2022.121093
17. Mei L., Wang H.G., Duan Q. *J. Phys.: Conf. Ser.* **2020**, *1605*, 012177. doi: 10.1088/1742-6596/1605/1/012177
18. Li J., Ma P.C., Chow W.S., To C.K., Tang B.Z., Kim J.-K. *Adv. Funct. Mater.* **2007**, *17*, 3207–3215. doi: 10.1002/adfm.200700065
19. Predtechenskiy M.R., Khasin A.A., Bezrodny A.E., Bobrenok O.F., Dubov D.Y., Muradyan V.E., *et al. Carbon Trends* **2022**, *8*, 100175. doi: 10.1016/j.cartre.2022.100175
20. Bekyarova E., Itkis M.E., Cabrera N., Zhao B., Yu A., Gao J., *et al. J. Am. Chem. Soc.* **2005**, *127*, 5990–5995. doi: 10.1021/ja0431531
21. Lee J., Stein I.Y., Devoe M.E., Lewis D.J., Lachman N., Kessler S.S., *et al. Appl. Phys. Lett.* **2015**, *106*, 053110. doi: 10.1063/1.4907608
22. Conley K., Karttunen A.J. *J. Phys. Chem. C* **2022**, *126*, 17266–17274. doi: 10.1021/acs.jpcc.2c03904
23. Curran S.A., Talla J., Dias S., Zhang D., Carroll D., Birx D. *J. Appl. Phys.* **2009**, *105*, 073711. doi: 10.1063/1.3073938
24. Singh I., Bhatnagar P.K., Mathur P.C., Kaur I., Bharadwaj L.M., Pandey R. *Carbon* **2008**, *46*, 1141–1144. doi: 10.1016/j.carbon.2008.04.013
25. Grossiord N., Kivit P.J.J., Loos J., Meuldijk J., Kyrylyuk A.V., van der Schoot P., *et al. Polymer* **2008**, *49*, 2866–2872. doi: 10.1016/j.polymer.2008.04.033
26. Barnes T.M., Blackburn J.L., van de Lagemaat J., Coutts T.J., Heben M.J. *ACS Nano* **2008**, *2*, 1968–1976. doi: 10.1021/nn800194u
27. Cao Q., Yu Q., Connell D.W., Yu G. *Clean Techn. Environ. Policy* **2013**, *15*, 871–880. doi: 10.1007/s10098-013-0581-y
28. Dalcanale F., Grossenbacher J., Blugan G., Gullo M.R., Brugger J., Tevaearai H., *et al. J. Eur. Ceram. Soc.* **2015**, *35*, 2215–2224. doi: 10.1016/j.jeurceramsoc.2015.02.016
29. Camilli L., Pisani C., Passacantando M., Grossi V., Scarselli M., Castrucci P., *et al. Appl. Phys. Lett.* **2013**, *102*, 183117. doi: 10.1063/1.4804385
30. Espinola A., Miguel P.M., Salles M.R., Pinto A.R. *Carbon* **1986**, *24*, 337–341. doi: 10.1016/0008-6223(86)90235-6
31. Probst N., Grivei E. *Carbon* **2002**, *40*, 201–205. doi: 10.1016/s0008-6223(01)00174-9
32. Stepina N.P., Galkov M.S., Predtechenskiy M.R., Bezrodny A.E., Kirienko V.V., Dvurechenskii A.V. *Mod. Electron. Mater*. **2019**, *5*, 21–26. doi: 10.3897/j.moem.5.1.39452
33. Mitina A.A., Redkin A.N., Yakimov E.E. *Fullerenes, Nanotubes and Carbon Nanostructures* **2020**, *28*, 112–117. doi: 10.1080/1536383x.2019.1680976
34. Kurochkin I.Y., Rudneva T.N., Ryzhkova G.G., Vinnik D.A., Yakimov E.E., Korepanov V.I. *Macroheterocycles* **2025**, *18*, 118–123. doi: 10.6060/mhc256568k
35. Korepanov V.I., Sedlovets D.M. *Mater. Res. Express* **2019**, *6*, 055317. doi: 10.1088/2053-1591/ab059c
36. Szybowicz M., Makowiecki J. *J. Mater. Sci.* **2011**, *47*, 1522–1530. doi: 10.1007/s10853-011-5940-7
37. Soliman H.S., El Nahass M.M., Farid A.M., Farag A.A.M., El Shazly A.A. *Eur. Phys. J. Appl. Phys.* **2003**, *21*, 187–193. doi:10.1051/epjap:2003003
38. Liao M.S., Kuo K.T. *Polym. J.* **1993**, *25*, 947–953. doi: 10.1295/polymj.25.947
39. Abe K., Saito H., Kimura T., Ohkatsu Y., Kusano T. *Makromol. Chem.* **1989**, *190*, 2693–2701. doi: 10.1002/macp.1989.021901103
40. Felmayer W., Wolf I. *J. Electrochem. Soc.* **1958**, *105*, 141. doi: 10.1149/1.2428778
41. Zhang H.-L., Li J.-F., Zhang B.-P., Yao K.-F., Liu W.-S., Wang H. *Phys. Rev. B* **2007**, *75*, 205407. doi: 10.1103/physrevb.75.205407
42. Ksenevich V.K., Seliuta D., Martūnas Z., Kašalynas I., Valušis G., Galibert J., *et al. Acta Phys. Pol., A* **2008**, *113*, 1039–1042. doi: 10.12693/aphyspola.113.1039
43. Nirmalraj P.N., Lyons P.E., De S., Coleman J.N., Boland J.J. *Nano Lett.* **2009**, *9*, 3890–3895. doi: 10.1021/nl9020914


*Received 21.05.2025*
*Accepted 15.10.2025*